

Clock Skew Compensation Algorithm Immune to Floating-Point Precision Loss

Kyeong Soo Kim, *Senior Member, IEEE*, and Seungyeop Kang

Abstract—We propose a novel clock skew compensation algorithm based on Bresenham’s line drawing algorithm. The proposed algorithm can avoid the effect of limited floating-point precision (e.g., 32-bit single precision) on clock skew compensation and thereby provide high-precision time synchronization even with resource-constrained sensor nodes in wireless sensor networks.

Index Terms—Clock skew compensation, Bresenham’s algorithm, time synchronization, floating-point arithmetic, wireless sensor networks.

I. INTRODUCTION

CLOCK skew compensation is an essential component of time synchronization in wireless sensor networks (WSNs), which provides a common time frame among network nodes [1]. Because typical clock skew compensation algorithms are involved with floating-point arithmetic, their performance on the platforms with lower computational resources—e.g., 32-bit single-precision floating-point format on resource-constrained WSN sensor nodes—is not up to the predicted performance from theories or simulation experiments [2].

To address the issue of the limited precision floating-point arithmetic in clock skew compensation, therefore, we propose a novel scheme based on Bresenham’s line drawing algorithm [3] immune to floating-point precision loss.

II. CLOCK MODELS

Without loss of generality, we confine our discussions to a network with one head node and one sensor node in this letter, where we describe the hardware clock T of the sensor node with respect to the reference clock t of the head node using the first-order affine clock model [4]:

$$T(t) = (1 + \epsilon)t + \theta, \quad (1)$$

where $\epsilon \in \mathbb{R}$ and $\theta \in \mathbb{R}$ denote the clock skew and offset, respectively; $(1 + \epsilon_i) \in \mathbb{R}_+$ in (1) is also called *clock frequency ratio* in the literature. Because we focus on the clock skew compensation, we simplify (1) by setting θ to 0 as follows:

$$T(t) = (1 + \epsilon)t. \quad (2)$$

Note that the time synchronization schemes based on the reverse two-way message exchange proposed in [5] are based

on the offset-free clock model of (2), where the clock offset is independently compensated for at the head node, while the sensor node only synchronizes the frequency of its logical clock to that of the reference clock.

Compensating for the clock skew from the hardware clock T in (2), we can obtain the logical clock \hat{t} of the sensor node—i.e., the estimation of the reference clock t given the hardware clock T —as follows: For $t_i < t \leq t_{i+1}$ ($i=0, 1, \dots$),

$$\hat{t}(T(t)) = \hat{t}(T(t_i)) + \frac{T(t) - T(t_i)}{1 + \hat{\epsilon}_i}, \quad (3)$$

where t_i is the reference time for the i th synchronization and $\hat{\epsilon}_i$ is the estimated clock skew from the i th synchronization.

The impact of the limited precision in floating-point arithmetic on clock skew compensation is investigated in [2]: The major finding is that the division of floating-point numbers in (3) incurs substantial precision loss at typical WSN platforms with 32-bit single precision. In case of the time synchronization scheme based on the reverse two-way message exchange [5], because the logical clock updates at sensor nodes in (3) requires accurate floating-point division and has a recursive nature, the impact of the precision loss on the logical clock is accumulated over time.

III. CLOCK SKEW COMPENSATION BASED ON BRESENHAM’S ALGORITHM

The modeling of hardware and logical clocks in Section II are based on the continuous-time affine clock model. In reality, however, clocks are discrete counters in digital communication systems [6]; timestamp values that are exchanged between a head and sensor nodes or recorded for events and measurements at sensor nodes in WSNs are based on the readings of discrete counters. The clock frequency ratio, too, can be estimated as the ratio of timestamp values.

Let $\frac{D}{A}$ be the inverse of a clock frequency ratio (i.e., $\frac{1}{1+\epsilon_i}$) estimated based on two positive integers D and A from the previous synchronization process in (3), where D and A represent interdeparture and interarrival times of packets or their cumulative sums [7]. Then, based on the well-known Bresenham’s line drawing algorithm [3], we can compensate for the clock skew as shown in Fig. 1¹ and map the sensor’s hardware clock to the head’s reference clock as follows: For

¹The coordinates are shifted by a pair of the initial values of hardware and logical clocks, e.g., $(T(t_i), \hat{t}(T(t_i)))$ in (3).

This work was supported in part by the Postgraduate Research Scholarships (under Grant PGRS1912001) and the Key Programme Special Fund (under Grant KSF-E-25) of Xi’an Jiaotong-Liverpool University.

K. S. Kim is with the Department of Communications and Networking, School of Advanced Technology, Xi’an Jiaotong-Liverpool University, Suzhou 215123, P. R. China (e-mail: Kyeongsoo.Kim@xjtlu.edu.cn).

S. Kang is with the Department of Mechatronics and Robotics, School of Advanced Technology, Xi’an Jiaotong-Liverpool University, Suzhou 215123, P. R. China (e-mail: S.Kang18@student.xjtlu.edu.cn).

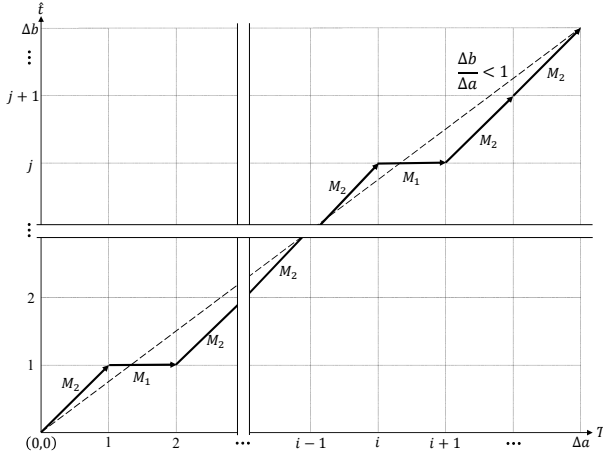


Fig. 1. Clock skew compensation based on Bresenham's line drawing algorithm [3] for the case of $\frac{\Delta b}{\Delta a} < 1$.

$\frac{D}{A} < 1$, we set Δa and Δb to A and D , respectively, and calculate ∇_i using the following recursive relation:²

$$\nabla_0 = 2\Delta b - \Delta a, \quad (4)$$

$$\nabla_{i+1} = \begin{cases} \nabla_i + 2\Delta b - 2\Delta a & \text{if } \nabla_i \geq 0, \\ \nabla_i + 2\Delta b & \text{otherwise.} \end{cases} \quad (5)$$

Then, from the origin and on, we determine each movement based on ∇_i :

$$\begin{cases} M_1 & \text{if } \nabla_i < 0, \\ M_2 & \text{otherwise,} \end{cases} \quad (6)$$

where M_1 is a horizontal movement and M_2 is a diagonal movement shown in Fig. 1. Lemma 1 shows that ∇_i is bounded.

Lemma 1. ∇_i satisfies the following inequality:

$$|\nabla_i| < 2\Delta a. \quad (7)$$

Proof: See Appendix A. ■

Unlike the line drawing, the skew compensation in our case does not need all the intermediate points between the origin and the point under consideration; we need only the y coordinate of a point given its x coordinate (e.g., j given i in Fig. 1), where x coordinate is the hardware clock T for an event or a measurement at the sensor node and y coordinate is its corresponding logical clock $\hat{t}(T)$. Therefore, we cannot use Bresenham's original algorithm as it is, especially when D and A are large and there are sparse events/measurements.

To extend Bresenham's algorithm for skew compensation, let's consider the example shown in Fig. 2, where the only valid path from $(0,0)$ to $(6,4)$ according to Bresenham's algorithm is indicated by black arrows while alternative paths are by gray arrows. Though the alternative paths are not useful for line drawing, they can reach the same destination and thereby provide the correct y coordinate. In fact, Lemma 1 shows that ∇_i in Bresenham's algorithm depends only on

²The case of $\frac{D}{A} > 1$ will be handled in Theorem 1, and the index starts from 0 to make mapping easier between ∇_i and the x coordinate of a point (e.g., ∇_0 is for $(0,0)$).

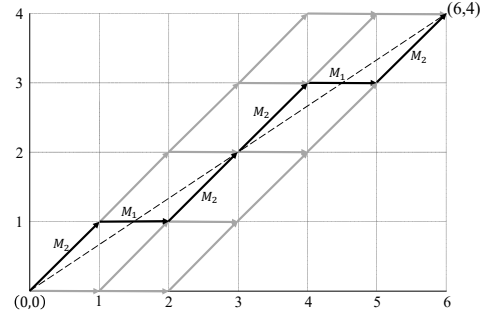


Fig. 2. Example of all possible paths from the origin to a given destination point based on M_1 and M_2 movements.

the number of M_2 , not the exact sequence of M_1 and M_2 , during the total i movements. Therefore, we extend ∇_i of Bresenham's algorithm to the points on all possible paths from the origin to a given destination of $(\Delta a, \Delta b)$ based on the two movements of M_1 and M_2 and define $\bar{\nabla}_i(j)$ as follows:

Definition 1. Given a destination point $(\Delta a, \Delta b)$, we define valid point set $\mathcal{V}(\Delta a, \Delta b)$ as a set of the points on a valid path from $(0,0)$ to $(\Delta a, \Delta b)$ according to Bresenham's algorithm.

Definition 2. Given a point $(i,j) \in \mathcal{V}(\Delta a, \Delta b)$, we define backward-reachable set $\mathcal{B}(i,j)$ as a set of the points that can reach (i,j) by any combination of the movements M_1 and M_2 as follows:

$$\mathcal{B}(i,j) \triangleq \{(k,l) | 0 \leq k < i, \max(0, k - \Delta a + \Delta b) \leq l \leq \min(k, j)\}. \quad (8)$$

Definition 3. For a point $(i,j) \in \mathcal{B}(\Delta a, \Delta b)$, we define $\bar{\nabla}_i(j)$ as follows:

$$\bar{\nabla}_i(j) \triangleq 2(i\Delta b - j\Delta a). \quad (9)$$

Note that $\bar{\nabla}_i(j) = \nabla_i, \forall (i,j) \in \mathcal{V}(\Delta a, \Delta b)$. Lemma 2 shows the property of $\bar{\nabla}_i(j)$ essential to the extension of Bresenham's algorithm to clock skew compensation:

Lemma 2. A point $(i,j) \in \mathcal{V}(\Delta a, \Delta b)$ is reachable from any point $(k,l) \in \mathcal{B}(i,j)$ if we apply (4)–(6) using $\bar{\nabla}(\cdot)$ instead of $\nabla(\cdot)$.

Proof: See Appendix B. ■

Now we can prove the main theorem for the clock skew compensation based on the extension of Bresenham's algorithm, which can eliminate the effect of precision loss on floating-point arithmetic:

Theorem 1. Given the hardware clock i , we can obtain its skew-compensated clock j as follows:

Case 1. $\frac{D}{A} < 1$: The skew-compensated clock j satisfies

$$i\frac{D}{A} - 1 < j < i\frac{D}{A} + 1. \quad (10)$$

Unless $i\frac{D}{A}$ is an integer, there are two values satisfying (10). Due to the effect of limited floating-point precision, however, we cannot know the exact value of $i\frac{D}{A}$. In this regard, (10) can be extended to include the effect of the precision loss:

$$i\frac{D}{A} - 1 - \varepsilon < j < i\frac{D}{A} + 1 + \varepsilon, \quad (11)$$

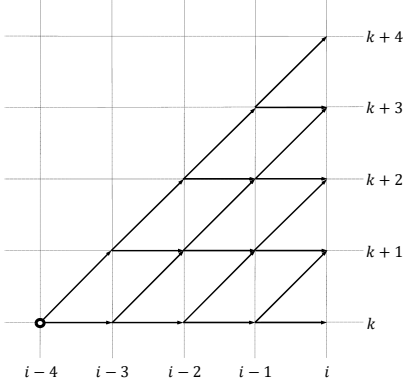


Fig. 3. Example of common starting points reaching all possible candidate points for the case of $\frac{\Delta b}{\Delta a} < 1$.

where $\varepsilon(>0)$ is the error due to the precision loss. Let $k, \dots, k+l$ be the candidate values of j satisfying (11). We determine j by starting from the point $(i-l, k)$ and applying Bresenham's algorithm with $\nabla_{i-l}(k)$ and on; j is determined by the y coordinate of the valid point whose x coordinate is i .

Case 2. $\frac{D}{A} > 1$: In this case, we can decompose the skew-compensated clock j into two components as follows:

$$j = i \frac{D}{A} = i + i \frac{D-A}{A}. \quad (12)$$

Now that $\frac{D-A}{A} < 1$, we can apply the same procedure of Case 1 to the second component in (12) by setting Δa and Δb to A and $D-A$, respectively. Let \bar{j} be the result from the procedure. The skew-compensated clock j is given by $i + \bar{j}$ as per (12).

Proof: See Appendix C. ■

In summary, the clock skew compensation algorithm described in Theorem 1 allows us to bound the correct skew-compensated clock given a hardware clock by (11) and search for it from a nearby starting point using the extension of Bresenham's algorithm based on $\nabla(\cdot)$. Fig. 3 illustrates an example of the starting point discussed in Theorem 1.

Note that the case of $\frac{D}{A} > 1$ is handled by setting Δa and Δb to D and A in Bresenham's original algorithm, where we need to find the skew-compensated clock j on the x -axis given the hardware clock i on the y -axis. The major issue is that there could be multiple points on the x -axis given a point in the y -axis (e.g., $(1, 1)$ and $(2, 1)$ in Fig. 1) due to the movement of M_1 . The algorithm described in Theorem 1 can avoid such an issue resulting from the change of the axes by unifying both cases with the same procedure for $\frac{D}{A} < 1$.

A. Numerical Examples

We apply the proposed algorithm to the representative cases whose results are summarized in Table I. We fix D to 1,000,000 and generate one million samples of A whose clock skews are uniformly distributed in the range of $[-100 \text{ ppm}, 100 \text{ ppm}]$ [8]. The value of ε is set to $1\text{E}-7$ based on the analysis in [2, Section 2]. Note that the minimum and the maximum values of the hardware clock correspond to 1 s and 1000 s, respectively, at a sensor node running TinyOS

TABLE I
RESULTS OF CLOCK SKEW COMPENSATION*.

Algorithm	Hardware clock	Compensation error [†]		
		Max.	Min.	Avg.
Single precision [‡]	1E6	0	0	0
	1E7	0	0	0
	1E8	1	-4	-2.0004
	1E9	44	-19	1.2382E1
Proposed	1E6	-1	-1	-1
	1E7	-1	-1	-1
	1E8	-1	-1	-1
	1E9	-1	-1	-1

* With $D=1,000,000$ and $\varepsilon=1\text{E}-7$.

[†] With respect to $\lfloor i \frac{D}{A} \rfloor$ based on double precision.

[‡] $\lfloor i \frac{D}{A} \rfloor$ based on single precision.

whose synchronization limit is $1 \mu\text{s}$ [9]. For the clock skew compensation by single and double-precision floating-point arithmetic, we round down the results to obtain integer values.

The results in Table I show that the clock skew compensation errors of the proposed algorithm with respect to the results based on double-precision floating-point arithmetic are bounded by -1 , while those of the single-precision algorithm begins to rapidly increase when the hardware clock is $1\text{E}8$. When we change rounding down to rounding off and rounding up for the results from double-precision and single-precision algorithms, we still obtain similar results where the clock skew compensation errors of the proposed algorithm are always bounded by ± 1 , which results from the difference in converting floating-point numbers to integers among the algorithms.

IV. CONCLUSIONS

In this letter, we have proposed a novel clock skew compensation algorithm immune to floating-point precision loss, where we extend Bresenham's algorithm to the points on all possible paths from the origin to the destination based on the movements of M_1 and M_2 and unify the two cases of $\frac{D}{A} < 1$ and $\frac{D}{A} > 1$ with a common procedure. Through numerical examples, we have also demonstrated that the proposed algorithm can compensate for clock skew without being affected by precision loss unlike the existing schemes based on floating-point divisions.

APPENDIX A PROOF OF LEMMA 1

Because $0 < \frac{\Delta b}{\Delta a} < 1$,

$$\begin{aligned} 0 &< \Delta b < \Delta a, \\ 0 &< 2\Delta b < 2\Delta a, \\ -\Delta a &< 2\Delta b - \Delta a < \Delta a, \\ \therefore -2\Delta a &< \nabla_0 < 2\Delta a. \end{aligned} \quad (13)$$

Let's assume $-2\Delta a < \nabla_i < 2\Delta a$ for $i \geq 0$.

Case 1. $\nabla_i \geq 0$:

$$\begin{aligned} 0 &\leq \nabla_i < 2\Delta a, \\ 2\Delta b - 2\Delta a &\leq \nabla_i + 2\Delta b - 2\Delta a < 2\Delta b. \end{aligned} \quad (14)$$

From (13), we have $-2\Delta a < 2\Delta b - 2\Delta a$ and $2\Delta b < 2\Delta a$. So we obtain

$$\begin{aligned} -2\Delta a &< \nabla_i + 2\Delta b - 2\Delta a < 2\Delta a, \\ \therefore -2\Delta a &< \nabla_{i+1} < 2\Delta a. \end{aligned} \quad (15)$$

Case 2. $\nabla_i < 0$:

$$\begin{aligned} -2\Delta a &< \nabla_i < 0, \\ 2\Delta b - 2\Delta a &< \nabla_i + 2\Delta b < 2\Delta b. \end{aligned} \quad (16)$$

Again, from (13), we have $-2\Delta a < 2\Delta b - 2\Delta a$ and $2D < 2A$. So we obtain

$$\begin{aligned} -2\Delta a &< \nabla_i + 2\Delta b < 2\Delta a, \\ \therefore -2\Delta a &< \nabla_{i+1} < 2\Delta a. \end{aligned} \quad (17)$$

(13)–(17) completes the proof by mathematical induction. ■

APPENDIX B PROOF OF LEMMA 2

We first show that $(i, j) \in \mathcal{V}(\Delta a, \Delta b)$ is reachable from $(i-1, l) \in \mathcal{B}(i, j)$, i.e., the points one step backward from it. Considering the movements of M_1 and M_2 , we could have at most two such points, i.e., $(i-1, j-1)$ and $(i-1, j)$.³

Case 1. $(i-1, j-1) \in \mathcal{V}(\Delta a, \Delta b)$: ∇_{i-1} should be equal to or greater than 0 so that we take M_2 and move to (i, j) . Now we have two subcases:

Case 1.1. Start from $(i-1, j-1)$: (i, j) can be reachable using $\bar{\nabla}_{i-1}(j-1)$ because $\bar{\nabla}_{i-1}(j-1) = \nabla_{i-1}$.

Case 1.2. Start from $(i-1, j)$: $\bar{\nabla}_{i-1}(j) = \bar{\nabla}_{i-1}(j-1) - 2\Delta a$, so we have

$$\begin{aligned} -2\Delta a &< \bar{\nabla}_{i-1}(j-1) < 2\Delta a \quad (\because \bar{\nabla}_{i-1}(j-1) = \nabla_{i-1}), \\ -4\Delta a &< \bar{\nabla}_{i-1}(j-1) - 2\Delta a < 0, \\ -4\Delta a &< \bar{\nabla}_{i-1}(j) < 0. \end{aligned} \quad (18)$$

Because $\bar{\nabla}_{i-1}(j) < 0$, we take M_1 and move to (i, j) .

Case 2. $(i-1, j) \in \mathcal{V}(\Delta a, \Delta b)$: ∇_{i-1} should be less than 0 so that we take M_1 and move to (i, j) . Again, we have two subcases:

Case 2.1. Start from $(i-1, j-1)$: $\bar{\nabla}_{i-1}(j-1) = \bar{\nabla}_{i-1}(j) + 2\Delta a$, so we have

$$\begin{aligned} -2\Delta a &< \bar{\nabla}_{i-1}(j) < 2\Delta a \quad (\because \bar{\nabla}_{i-1}(j) = \nabla_{i-1}), \\ 0 &< \bar{\nabla}_{i-1}(j) + 2\Delta a < 4\Delta a, \\ 0 &< \bar{\nabla}_{i-1}(j-1) < 4\Delta a. \end{aligned} \quad (19)$$

Because $\bar{\nabla}_{i-1}(j-1) > 0$, we take M_2 and move to (i, j) .

Case 2.2. Start from $(i-1, j)$: (i, j) can be reachable using $\bar{\nabla}_{i-1}(j)$ because $\bar{\nabla}_{i-1}(j) = \nabla_{i-1}$.

Now we assume that $(i, j) \in \mathcal{V}(\Delta a, \Delta b)$ is reachable from $(i-k, l) \in \mathcal{B}(i, j)$ for $k \geq 1$, i.e., the points k step backward from it. Because in general we can move to $(i-k, l) \in \mathcal{B}(i, j)$ from the points $k+1$ step back from (i, j) by taking either M_1 or M_2 , we consider only two special boundary cases of $(\Delta a - \Delta b, 0)$ and $(\Delta b, \Delta b)$ ⁴ to check whether the movement from those points still belongs to $\mathcal{B}(i, j)$.

Case 1. $(i-k-1, l) = (\Delta a - \Delta b, 0)$: $\bar{\nabla}_{\Delta a - \Delta b}(0) = 2\Delta b(\Delta a - \Delta b) > 0$, so we take M_2 and the next point belongs to $\mathcal{B}(i, j)$.

Case 2. $(i-k-1, l) = (\Delta b, \Delta b)$: $\bar{\nabla}_{\Delta b}(\Delta b) = 2\Delta b(\Delta b - \Delta a) < 0$, so we take M_1 and the next point belongs to $\mathcal{B}(i, j)$.

This completes the proof by mathematical induction. ■

APPENDIX C PROOF OF THEOREM 1

Here we prove only Case 1 because Case 2 follows from Case 1 and is just its application.

Case 1. $\frac{D}{A} < 1$: If $(i, j) \in \mathcal{V}(\Delta a, \Delta b)$, we obtain the following from Lemma 1 and Definition 3:

$$\begin{aligned} -2\Delta a &< \bar{\nabla}_i(j) < 2\Delta a, \\ -2\Delta a &< 2(i\Delta b - j\Delta a) < 2\Delta a, \\ -2A &< 2(iD - jA) < 2A \quad (\because \Delta a = A, \Delta b = D). \end{aligned} \quad (20)$$

Hence (10). If $i\frac{D}{A}$ is not an integer, it is clear from (10) that there are two values satisfying the inequality. If we also include the effect of the precision loss, there could be even more values satisfying the extended inequality of (11).

Let $k, \dots, k+l$ be those values satisfying (11). Because $(i-l, k)$ belongs to $\bigcap_{m=0}^l \mathcal{B}(i, k+m)$ as per (8), we can reach from $(i-l, k)$ to a valid point—i.e., one of $(i, k), \dots, (i, k+l)$ —by applying Bresenham's algorithm with $\bar{\nabla}_{i-l}(k)$ by Lemma 2. ■

REFERENCES

- [1] Y.-C. Wu, Q. Chaudhari, and E. Serpedin, "Clock synchronization of wireless sensor networks," *IEEE Signal Process. Mag.*, vol. 28, no. 1, pp. 124–138, 2011.
- [2] X. Huan and K. S. Kim, "On the practical implementation of propagation delay and clock skew compensated high-precision time synchronization schemes with resource-constrained sensor nodes in multi-hop wireless sensor networks," *Computer Networks*, vol. 166, pp. 1–8, Jan. 2020.
- [3] J. E. Bresenham, "Algorithm for computer control of a digital plotter," *IBM Systems Journal*, vol. 4, no. 1, pp. 25–30, 1965.
- [4] R. T. Rajan and A.-J. van der Veen, "Joint ranging and clock synchronization for a wireless network," in *Proc. CAMSAP 2011*, Dec. 2011, pp. 297–300.
- [5] K. S. Kim, S. Lee, and E. G. Lim, "Energy-efficient time synchronization based on asynchronous source clock frequency recovery and reverse two-way message exchanges in wireless sensor networks," *IEEE Trans. Commun.*, vol. 65, no. 1, pp. 347–359, Jan. 2017.
- [6] B. Etzlinger, N. Palaoro, W. Haselmayr, B. Rudić, and A. Springer, "Timestamp free synchronization with sub-tick accuracy in the presence of discrete clocks," *IEEE Trans. Wireless Commun.*, vol. 16, no. 2, pp. 771–783, Feb. 2017.
- [7] K. S. Kim, "Asynchronous source clock frequency recovery through aperiodic packet streams," *IEEE Commun. Lett.*, vol. 17, no. 7, pp. 1455–1458, Jul. 2013.
- [8] Texas Instruments, "Selection and specification of crystals for Texas Instruments USB 2.0 devices," *Application Report*, Dec. 2002, accessed: 25 August 2021. [Online]. Available: <https://www.ti.com/lit/an/slla122/slla122.pdf>
- [9] TinyOS. [Online]. Available: <https://github.com/tinyos/tinyos-main>

³It is possible that $(i-1, j) \notin \mathcal{B}$ (e.g., (1, 1) in Fig. 2).

⁴See the points (2, 0) and (4, 4) in Fig. 2 as an example.